Fabrication of Cu₂ZnSnS₄ films by sulfurization of Cu/ZnSn/Cu precursor layers in sulfur atmosphere for solar cells

R.B.V. Chalapathy, Gwang Sun Jung, Byung Tae Ahn*

Department of Materials Science and Engineering, Korea Advanced Institute of Science and Technology, 291 Daehak-ro, Yuseong-gu, Daejeon 305-701, South Korea

ABSTRACT

Cu₂ZnSnS₄ (CZTS) absorbers were grown by sulfurization of Cu/ZnSn/Cu precursors in sulfur atmosphere. The reaction mechanism of CZTS formation from the precursor was analyzed using XRD and Raman spectroscopy. The films with a single phase CZTS were formed at 560 and 580 °C by sulfurization for 30 min. The film grown at 560 °C showed bi-layer morphology with grooved large grains on the top and dense small grains near the bottom of the film. On the other hand, the film grown at 580 °C showed large grains with grooves that are extended from surface top to bottom of the film. The solar cell fabricated with the CZTS film grown at 560 °C showed the best conversion efficiency of 4.59% for 0.44 cm² with $V_{oc}=0.545$ V, $J_{sc}=15.44$ mA/cm², and FF=54.6. We found that further improvement of the microstructure of CZTS films can increase the efficiency of CZTS solar cells.

© 2011 Elsevier B.V. All rights reserved.

1. Introduction

Cu₂ZnSnS₄ (CZTS) is considered a promising material as an absorber for thin film solar cells due to its suitable electro-optical properties such as direct band gap of 1.4–1.5 eV, which is the optimum band gap for high efficiency solar cells, p-type conductivity, and high absorption coefficient of over 10^4 cm^{-1} [1]. In addition to this CZTS's constituent elements, such as Zn and Sn, are more abundant and less expensive than In and Ga. CZTS crystallizes in a Kesterite structure, which can be obtained by substituting half of the indium with Zn and half with Sn in the chalcopyrite CuInS₂ structure. Recently Todorov et al. [2] achieved 9.66% efficient solar cells based on Cu₂ZnSn(SSe)₄ absorbers obtained by the solution process, demonstrating the potential of these absorbers. CZTS thin films were grown with various methods such as co-evaporation [3,4], RF sputtering and vapor phase sulfurization [5], electro plating and sulfurization [6,7], RF sputtering [8], hybrid sputtering [9], reactive sputtering [10], nanoparticles [11,12], and spray pyrolysis [13,14].

Among the various methods, co-evaporation and the two-step process have shown better performances with 4.1 and 6.67% efficiencies, respectively [4,6]. In the process with 6.67% efficiency, a metal or sulfur containing precursor layer is converted to CZTS by annealing in elemental sulfur vapor or H₂S. Typically, the metallic precursors are deposited by sputtering, electron beam, or electro plating methods with various combinations such as stacked or co-sputtered Cu/Zn/Sn layers. When staked layers are deposited using elemental metals the Sn droplets form on the Zn film, leading to inhomogeneous composition in the CZTS films [15]. One possible way to avoid this is to use alloy targets. The process times for the sulfurization are in the range of 3–8 h in H₂S to get homogeneous CZTS absorbers for device fabrication [5,6]. However, there is no clear understanding of the process conditions required for rapid growth of homogenous CZTS absorbers by sulfurization of metallic precursors. In order to grow good quality CZTS films by rapid thermal annealing it is necessary to understand the growth mechanism of CZTS films. The objective of this work is to optimize the process conditions to grow CZTS films with large grains and uniform composition for solar cell applications.

Here, we report on CZTS films grown by two-step sulfurization process. A precursor consisting of a Cu/Zn₆₀Sn₄₀/Cu layer was deposited by DC magnetron sputtering and was sulfurized in elemental sulfur vapor, which is less toxic than H₂S. Ex-situ XRD and Raman measurements on samples taken during the temperature ramping reveal that the formation of CZTS films was completed during the substrate ramping in ~6–7 min. A solar cell with the best conversion efficiency of 4.59% was obtained with the CZTS absorber grown at 560 °C for 30 min with the above process.

2. Experimental

CZTS thin films were grown by the sulfurization process. Metal precursors with the Cu/ZnSn/Cu sequence were deposited on 5 × 5 cm² Mo coated soda lime glass substrates by DC sputtering

* Corresponding author. Tel.: +82 42 350 4220; fax: +82 42 350 3310.
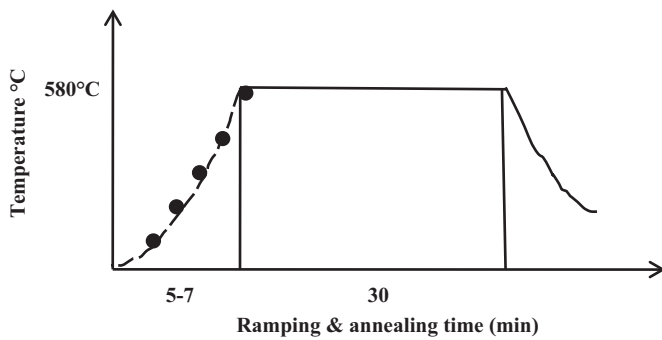E-mail address: btahn@kaist.ac.kr (B.T. Ahn).

Fig. 1. Temperature–time profile of sulfurization process.

at RT. The precursors were deposited under sputtering powers of 80 and 20 W for Cu and ZnSn(60:40 at%) sputtering targets, respectively, at the working pressure of 2 mTorr in Ar atmosphere. The ratio of Cu/(Zn+Sn) in the precursors was kept to 0.9 by controlling the thickness of Cu. The total thickness of the precursor was approximately 630 nm. The precursors were converted into CZTS films by annealing in S vapor. Sulfurization was carried out using a tubular quartz furnace, which was heated externally with halogen lamps. The precursors, with dimensions of 2.5×5 cm^2, and 500 mg of sulfur were placed in a graphite box, which was then inserted into the furnace. The precursors were annealed at 560 and 580 °C for 30 min at a ramping rate of 100 °C/min. The temperature versus time profile used in this study is shown in Fig. 1. The profile is similar to one used by Siemer et al. [16]. In order to understand the growth mechanism during temperature ramping, the process was interrupted intentionally at a specific ramping temperature (270, 370, 470, 530, and 580 °C within 7 min marked as dark circles in Fig. 1) and the samples were allowed to cool down to room temperature naturally.

The phases present in the as-deposited precursor and in the sulfurized CZTS films were identified with X-ray diffraction pattern and Raman spectroscopy. The XRD measurements were carried out using a Rigaku thin film diffractometer; Raman spectroscopy measurements were carried out with a Horiba Jobin Yvon LabRam High Resolution Raman spectrometer equipped with an Ar laser with excitation wavelength of 514.5 nm. The cross-sectional morphology and composition of the films were analyzed with a FEI NOVA 230 field emission scanning electron microscope (FESEM), and energy dispersive spectroscopy (EDS). The depth profiles of the films were measured using a Perkin Elmer Auger electron spectroscope. The optical transmittance of the film was measured with a Shimadzu UV-3101 PC spectrophotometer.

3. Results and discussion

3.1. CZTS formation

In order to understand the formation of CZTS films by sulfurization and to optimize the growth conditions in our experiments, the samples were taken out during ramping up of temperature to 580 °C and were analyzed with XRD and Raman measurements. Fig. 2 shows the XRD patterns of the as deposited precursor and of the samples obtained at various temperatures during the temperature ramping. The as deposited precursor consists of metal elements such as Zn and Sn and binary alloys such as Cu$_6$Sn$_5$, Cu$_3$Sn, and CuZn, indicating that Cu atoms diffuse into the ZnSn films during the sputtering process, resulting in the formation of binary inter-metallic phases. At 270 °C, peak positions corresponding to binary sulfide phases such as Cu$_2$S, SnS$_2$, and sulfur peaks were observed. At 370 °C the sample consists of
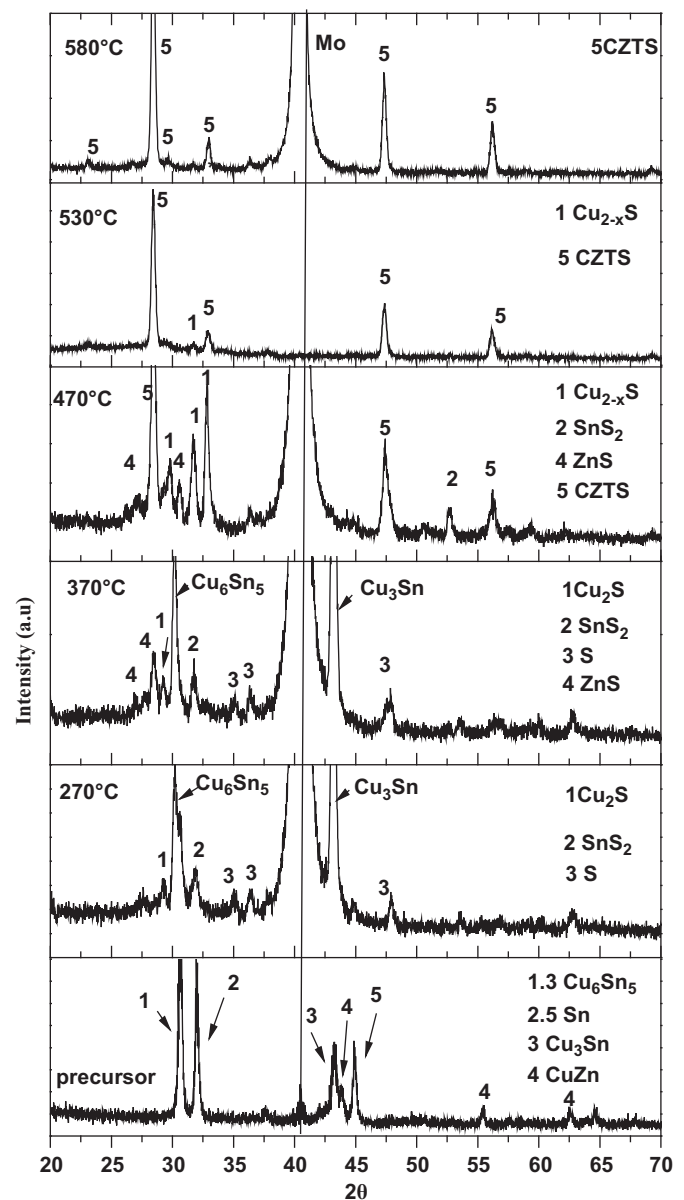

Fig. 2. XRD patterns of precursor and CZTS samples taken at various temperatures during temperature ramping in S atmosphere.

metallic phases Cu$_6$Sn$_5$, Cu$_3$Sn in addition to binary sulfides phases. For the sample taken at 470 °C a new peak at 28.53° that corresponds to the CZTS phase appears, indicating that CZTS forms at as low as 470 °C also consists of ZnS, CuS, and Cu$_{2-x}$S phases in the sample. At this temperature all the metallic phases disappeared, suggesting that these phases were converted into SnS$_2$, ZnS, and Cu$_{2-x}$S phases. At 530 °C, the CZTS phase becomes the predominant phase and a weak Cu$_2$S peak remains. At 580 °C, the CZTS peaks are sharp and well defined. No Cu$_2$S peak is observed. We found that the CZTS phase forms at as low as 470 °C and the reaction is completed in about 7 min of ramping to 580 °C in S atmosphere. The fast reaction suggests that the formation occurs with the help of liquid melt.

In order to support the XRD results, Raman measurements were carried out on the above samples. Fig. 3 shows the Raman spectra of the samples obtained at various temperatures during the temperature ramping. The samples taken at 270, 370, and 470 °C show a very strong peak positioned at 476 cm^{-1}, which is attributed to the presence of the Cu$_2$S phase. In these spectra no

other peaks corresponding to SnS_2, ZnS, or Cu_2SnS_3 were observed. The sample at 470 °C shows a new peak positioned at 338 cm^{-1}, which is assigned to the CZTS phase. At 530 and 580 °C the Raman spectra clearly show peak positions at 289 cm^{-1} and 338 cm^{-1}, respectively, corresponding to the CZTS phase [17].
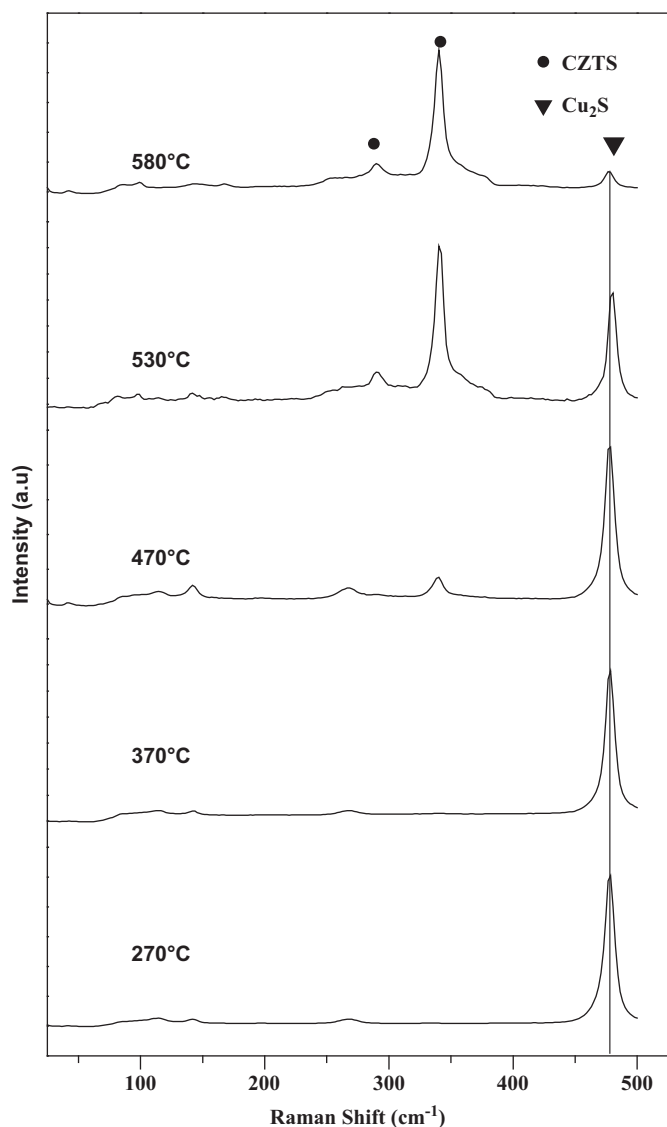

Fig. 3. Raman spectra of the CZTS samples taken at various temperatures during temperature ramping in S atmosphere.

The low intensity of the Cu_2S peak at 580 °C suggests that the Cu_2S phase is fully consumed in the formation of the CZTS film.

From the above XRD and Raman measurements, it is confirmed that the formation of CZTS can be completed even during the time of temperature ramping to 580°C. It is known that the CZTS phase forms from a solid state reaction of ternary Cu_2SnSn_3 and ZnS or directly from the binary phases of Cu_2S–SnS_2–ZnS without the intermediate compound Cu_2SnS_3 [18]. The XRD measurements of samples taken at 270 and 370 °C confirmed the presence of binary Cu_2S, SnS_2 and ZnS phases. Raman spectra showed no ternary phases such as Cu_2SnS_3, Cu_4SnS_4, and Cu_4SnS_6 in the samples, but only the Cu_2S phase exists even at higher temperatures. It is known that the formation of $Cu_{2-x}S$ phases is a highly sulfur pressure dependent [19]. In our experiment with closed chamber and fixed amount of sulfur only the temperature will determine the vapor pressure of sulfur (1–4 mbar), so during temperature ramping all Cu–S phases can form according to the Cu–S phase diagram [20]. The Digenite $Cu_{2-x}S$ is highly cation conducting phase [21] that provides Zn and Sn exchange leading to the formation of CZTS; it is also known as that $Cu_{2-x}S$ acts as a flux during the growth of CIS and CIGS [22–24]. Similarly, in CZTS film growth, $Cu_{2-x}S$ may assist film formation via liquid assisted grain growth, resulting in large grains and compact CZTS films. Both XRD and Raman measurements on the sample at 470 °C show the formation of CZTS phase in addition to $Cu_{2-x}S$ phase, also consistent with the Raman spectrum of the sample at 580 °C, where the intensity of the Raman peak at 338 cm^{-1} is increased from 116 (530 °C) to 1000 counts at 580 °C, whereas the intensity of the $Cu_{2-x}S$ peak decreased from 5000 (270 °C) to164 counts (580 °C), which clearly shows consumption of the $Cu_{2-x}S$ phase after temperature ramping. From the above results our study confirms that the CZTS phase is formed from the direct reaction among the binary sulfide phases, which is in agreement with the one of the reactions proposed by Hergert and Hock [18]. However, the presence of SnS_2 also induces the crystallization of CZTS. Schurr et al. showed from in-situ X-ray measurements that the re-formation of the 4H–SnS_2 melt phase from Cu_4SnS_6 at 840 K and the presence of this melt during crystallization of CZTS enhance the grain sizes of the films [25]. Our results reveal that growing CZTS thin films in the presence of $Cu_{2-x}S$ flux may be advantageous, which may result in large grains and dense films.

3.2. CZTS films

In the following experiments the process time is fixed at 30 min in order to get uniform and homogeneous CZTS films. Fig. 4(a) shows the XRD patterns of the CZTS sulfurized at 560 and 580 °C for 30 min. The patterns reveal that both films have a
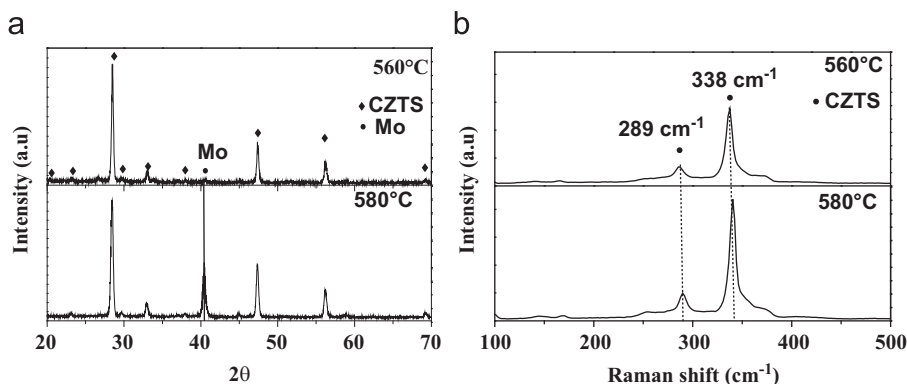

Fig. 4. (a) XRD patterns and (b) Raman spectra of the CZTS films grown at 560 and 580 °C for 30 min.
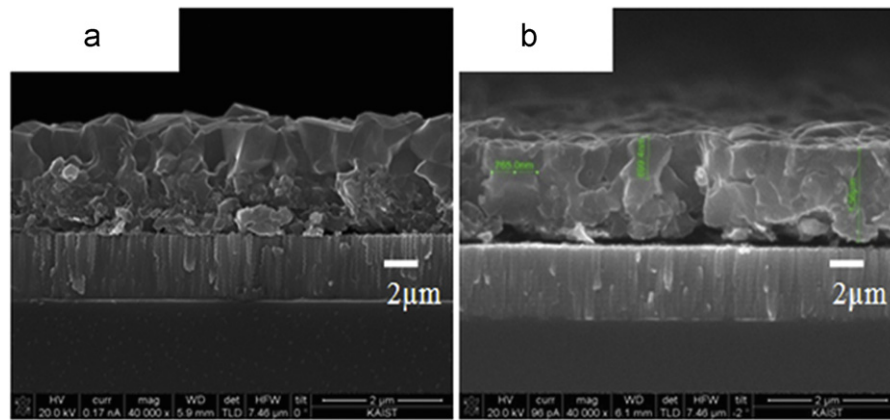
Fig. 5. Cross-sectional morphologies of the CZTS films grown at (a) 560 °C and (b) 580 °C for 30 min.

Table 1
Composition of the CZTS films grown at 560 and 580 °C for 30 min.

Precursor	Temperature (°C)	Cu	Zn	Sn	S	Cu/Zn$^+$Sn	Zn/Sn	S/M
(a) Cu/ZnSn/Cu	560	19.27	16.8	11.56	52.38	0.67	1.45	1.09
(b) Cu/ZnSn/Cu	580	23.64	12.21	12.28	51.87	0.96	0.99	1.08

Kesterite CZTS phase and are polycrystalline in nature. The Cu$_2$S peak shown during the ramping experiments is not observed after 30 min sulfurization. The Raman spectra of the above sulfurized films are shown in Fig. 4(b). Both spectra show peaks positioned at 289 cm^{-1} and 338 cm^{-1}, which were assigned to bulk CZTS [17]. Note that no Cu$_2$S phase is observed at 560 °C or 580 °C, indicating that the film is completely converted to CZTS after 30 min sulfurization.

Fig. 5 shows the cross-sectional morphologies of the CZTS films grown at 560 and 580 °C with Mo/ZnSn/Cu precursor. The thicknesses of the films are 1.9 and 1.55 μm, respectively. The film grown at 560 °C shows a double layer structure that consists of grooved large grains at the top and dense small grains at the bottom of the film. The film grown at 580 °C shows large grains that extend through the film and large voids at the CZTS/Mo interface. Even though the films consist of voids at the interface the overall adhesion of the films is good enough to fabricate CZTS solar cells. The pores and voids in the films can act as a shunting path in the devices. The grain sizes of our film were in the range 300–700 nm at the top of the film and 100–200 nm at the bottom of the film; on the other hand grain sizes as large as 14 μm in diameter were obtained by Ennaoui et al. probably due to their long process duration of 8 h in H$_2$S atmosphere [6].

The composition of films grown at 560 and 580 °C for 30 min is given in Table 1. The precursors are Cu poor with a Cu/(Zn+Sn) ratio of 0.9. The S/metal ratio is greater than 1 in the films, indicating that sulfur is sufficiently incorporated into the films. The film obtained at 560 °C shows a Cu poor and Zn rich composition with Cu/(Zn+Sn)=0.67 and Zn/Sn=1.45, whereas the film grown at 580 °C shows a slightly Cu poor composition with Zn/Sn=1. In general, CZTS solar cells fabricated with Cu poor and Zn rich composition have shown high conversion efficiencies [5]. The CZTS films grown at 560 and 580 °C have different compositions even though the precursor compositions are the same, which suggests that sulfurization temperature, in addition to the microstructure, has a strong influence on the composition of the films.

Fig. 6 shows Auger depth profiles of sulfurized CZTS films grown at (a) 560 and (b) 580 °C. The film grown at 560 °C shows that Zn, Sn, and S are rich in the back region. This behavior is generally observed in the sulfurized CZTS films due to ZnS precipitates in the films [6]. The film grown at 580 °C shows that Cu, Zn, Sn, and S are distributed uniformly throughout the thickness of the film. The presence of quasi-Cu$_{2-x}$S liquid phase during the fast ramping may assist rapid diffusion of Zn and Sn. At higher temperature the presence of this phase may enhance the higher diffusion of cations, which could lead to homogeneous CZTS film. It is well known in CIGS film growth that the presence of quasi-liquid Cu$_{2-x}$Se phase enhances the diffusion of In and Ga into the CIGS film [26,27]. Similar behavior can be attributed to diffusion of Zn and Sn into CZTS during film growth. This shows that the sulfurization temperature has a strong influence on the distribution of the elements in the CZTS films.

Fig. 7(a) shows the optical transmittance spectrum of the CZTS film grown at 580 °C for 30 min. From the transmittance spectrum the absorption coefficient α was evaluated using the relation $\alpha = -\ln(T)/t$, where T is the transmittance of the film and t is the film thickness. The absorption coefficient of the film is in the order of 10^4 cm^{-1}. The band gap of the films is determined by extrpolating the linear region of the α^2 versus $h\nu$ (photon energy) curve to the intercept of the $h\nu$ axis, as can be seen in Fig. 7(b). The band gap of the film is determined to be 1.51 eV. This value is in good agreement with the reported direct band gap of CZTS [4]. The low transmittance (20%) in the long wavelength indicates that the film contains other scattering defects in the bulk CZTS, suggesting that our film is not of good quality.

The Hall measurement was performed on this sample. The carrier concentration of the film and the resistivity of the film are 6.2×10^{16} cm^{-3} and 0.2 Ω cm, respectively. The optical and electrical properties demonstrate that CZTS films grown by sulfurization can be used as absorbers in thin film solar cells.

3.3. Solar cells

Solar cells using the above CZTS films were fabricated in the Al/Al–ZnO/i-ZnO/CdS/CZTS/Mo/glass configuration; 70 nm CdS was deposited by chemical bath deposition and 50 nm intrinsic ZnO and Al doped n-ZnO were deposited by RF sputtering. Finally, Al as a top contact was deposited by electron beam evaporation using an aperture mask. I–V measurements were performed on
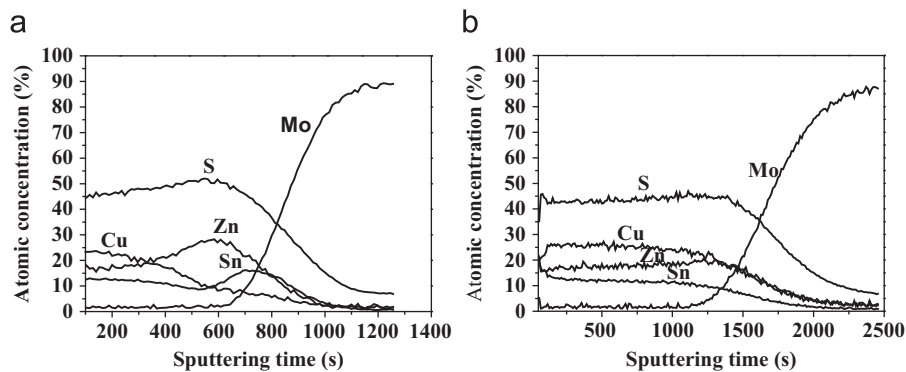
Fig. 6. AES depth profiles of the sulfurized CZTS films: (a) 560 °C and (b) 580 °C for 30 min.
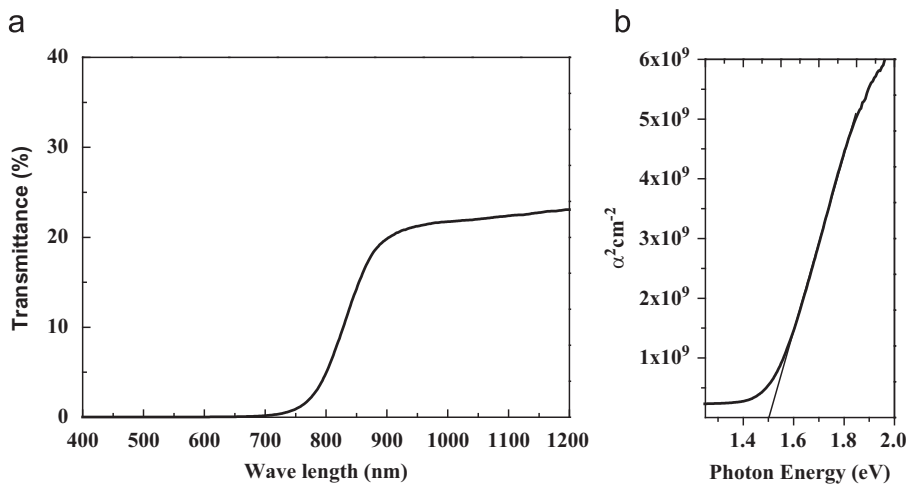

Fig. 7. (a) Optical transmittance spectrum and (b) plot of α^2 versus $h\nu$ of the CZTS film grown at 580 °C for 30 min in sulfur atmosphere.

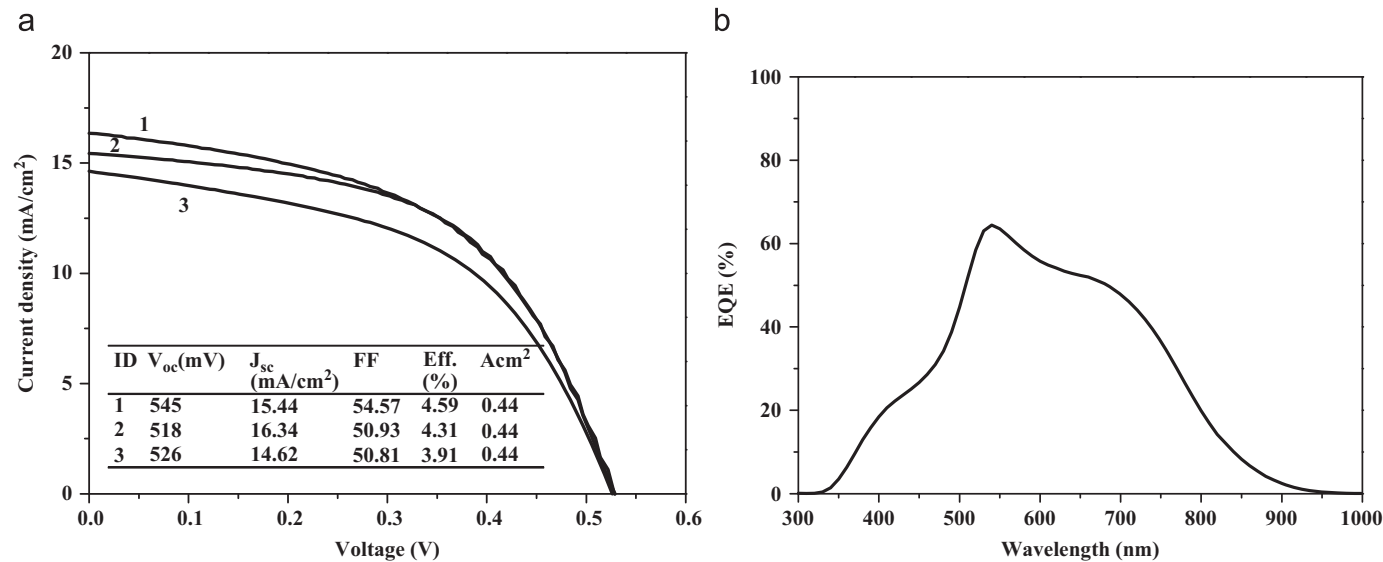| ID	V$_{oc}$(mV)	J$_{sc}$ (mA/cm^2)	FF	Eff. (%)	Acm^2
1	545	15.44	54.57	4.59	0.44
2	518	16.34	50.93	4.31	0.44
3	526	14.62	50.81	3.91	0.44

Fig. 8. (a) Current–voltage characteristics of the solar cells fabricated with CZTS absorber grown at 560 °C and (b) external quantum efficiency curve of the best solar cell.

the solar cell under 1.5AM (1000 W/m^2) irradiation with a Mac Science solar simulator. The external quantum efficiency was measured with PV measurements using a spectral photocurrent meter. The solar cells fabricated with the film grown at 560 °C for 30 min showed the best conversion efficiency of 4.59% for 0.44 cm^2 with an open circuit voltage of 0.545 V, short circuit current density of 15.44 mA/cm^2, and fill factor of 54.57, as shown

in the illuminated current–voltage characteristics of the solar cells in Fig. 8(a). The other two cells showed conversion efficiencies of 3.91% and 4.31%. The composition of the film grown at 560 °C is Cu/(Zn+Sn)=0.67 and Zn/Sn =1.45, which is highly Cu poor and Zn rich compared to the best reported CZTS (6.67%) solar cell (with Cu/(Zn+Sn)=0.85, Zn/Sn= 1.25) [5]. On the other hand solar cells fabricated with absorbers grown at 580 °C have an

efficiency of 0.6 %, due to voids and pores in the film that act as a shunting path in the devices.

The good performance of the cell with CZTS film grown at 560 °C is due to the dense microstructure at the Mo/CZTS interface, as seen in Fig. 4(a). The better performance is also due to the Cu-poor and Zn-rich composition. The external quantum efficiency of the best solar cell is given in Fig. 8(b); it shows a maximum quantum efficiency of about 65% at 520 nm. At shorter wavelengths the quantum efficiency is decreased due to absorption by the CdS layer; at higher wavelengths the curve showed a long tail from 700 nm, indicating small electron diffusion length. The band gap, estimated from the long wavelength cutoff, is about 1.46 eV, which is in agreement with the value obtained from optical measurements for absorber grown at 580 °C. The quantum efficiency curve shows that further enhancement in collection efficiency is possible by improving the electronic quality of the CZTS absorber and optimizing the CdS thickness .

4. Conclusions

We have grown CZTS absorbers by sulfurization of Cu/ZnSn/Cu precursors. XRD and Raman analyses of samples taken during the temperature ramping confirm that the formation of CZTS is completed in about 7 min at a 100 °C/min heating rate. CZTS films obtained at 560 and 580 °C for 30 min exhibited the Kesterite structure. Sulfurization temperature has a strong influence on the microstucture and distribution of elements in the films. The film grown at 560 °C exhbited bi-layer morphology compared to the film grown at 580 °C. AES depth profiles illustrate that the film grown at 560 °C is more inhomogeneous than the film obtained at 580 °C. Solar cells fabricated with CZTS absorbers grown at 560 °C for 30 min showed the best conversion efficiency of 4.59% for 0.44 cm^2 under standard AM 1.5 conditions. To our knowledge 4.59% is the highest efficiency for a CZTS solar cell obtained from absorbers grown with metal precursors and sulfurization in sulfur vapor. Further work will be focused on optimization of the temperature–time profile of sulfurization to get large grain morphology without pores and homogeneous CZTS absorbers for fabrication of high efficiency CZTS thin film solar cells.

Acknowledgments

References

[1] K. Ito, T. Nakazawa, Electrical and optical properties of stannite-type quaternary semiconductor thin films, Jpn. J. Appl. Phys. 27 (1988) 2094–2097.
[2] T.K. Todorov, K.B. Reuter, D.B. Mitizi, High-efficiency solar cell with earth-abundant liquid-processed absorber, Adv. Mater. 22 (2010) 1–4.
[3] T.M. Friedlmeier, N. Weiser, T. Walter, H. Dittrich, H.W. Schock, Heterojunctions based on Cu$_2$ZnSnS$_4$ and Cu$_2$ZnSnSe$_4$ thin films, in: Proceedings of the 14th EPVSEC Conference, P4B.10, 1997, pp. 1242–1245.
[4] B.A. Schubert, B. Marsen, S. Cinque, T. Unold, R. Klenk, S. Schorr, H.W. Schock., Cu$_2$ZnSnS$_4$ thin film solar cells by fast co-evaporation, Prog. Photovolt: Res. Appl. 19 (2011) 93–96.
[5] H. Katagiri, K. Jimbo, W. Shwe Maw, K. Oishi, M Yamazaki, H. Araki, A. Takeuchi, Development of CZTS based thin film solar cells, Thin Solid Films 517 (2009) 2455–2460.
[6] A. Ennaoui, M. Lux-Steiner, A. Weber, D. Abou-Ras, I. Kötschau, H.W. Schock, R. Schurr, A. Hölzing, S. Jost, R. Hock, T. Voß, J. Schulze, A. Kirbs, Cu$_2$ZnSnS$_4$ thin film solar cells from electroplated precursors: novel low cost perspective, Thin Solid Films 517 (2009) 2511–2514.
[7] J.J. Scragg, D.M. Berg, P.J. Dale, A 3.2% efficient Kesterite device from electrodeposited stacked layers, J. Electroanal. Chem. 646 (1–2) (2010) 52–59.
[8] J. Seol, S. Lee, J. Lee, H. Nam, K. Kim, Electrical and optical properties of Cu$_2$ZnSnS$_4$ thin films prepared by rf sputtering process, Sol. Energy Mater. Sol. Cells 75 (2003) 155–162.
[9] T. Tanaka, T. Nagatomo, D. Kawasaki, M. Nishio, Q. Guo, A. Wakahara, A. Yoshida, H Ogawa, Preparation of Cu$_2$ZnSnS$_4$ thin films by hybrid sputtering, J. Phys. Chem. Solids 66 (2005) 1978–1981.
[10] F. Liu, Y. Li, K. Zhang, B. Wang, C. Yan, Y. Lai, Z. Zhnag, J. Lie, Y. Lu, In situ growth of Cu$_2$ZnSnS$_4$ thin films by reactive magnetron co-sputtering, Sol. Energy Mater. Sol. Cells 94–12 (2010) 2431–2434.
[11] Q. Guo, H.W. Hillhouse, R. Agrawal, Synthesis of Cu$_2$ZnSnS$_4$ nano crystal ink and its use for solar cells, J. Am. Chem. Soc. 131 (2009) 11672–11673.
[12] C. Steinhagen, M.G. Phatani, V. Akhvan, B. Goodfellow, B. Koo, A. Korgel, Synthesis of Cu$_2$ZnSnS$_4$ nanocrystals for use in low-cost photovoltaics, J. Am. Chem. Soc. 131 (2009) 12554–12555.
[13] N. Nakayama, K. Ito, Sprayed films of stannite Cu$_2$ZnSnS$_4$, Appl. Surf. Sci. 92 (1996) 171–175.
[14] N. Kamoun, H. Bouzouita, B. Rezig, Fabrication and characterization of Cu$_2$ZnSnS$_4$ thin films deposited by spray pyrolysis technique, Thin Solid Films 515 (2007) 5949–5952.
[15] H. Araki, A. Mikaduki, Y. Kubo, T. Sato, K. Jimbo, W.H. Maw, H. Katagiri, M. Yamazaki, K. Oishi, A. Takeuchi, Preparation of Cu$_2$ZnSnS$_4$ thin films by sulfurization of stacked metallic layers, Thin Solid Films 517 (2008) 1457–1460.
[16] K. Siemer, J. Klaer, I. Luck, J. Bruns, R. Klenk, D. Braunig, Efficient CuInS$_2$ solar cells from rapid thermal process, Sol. Energy Mater. Sol. Cells 67 (2001) 159–166.
[17] P.A. Fernades, P.M.P. Salome, A.F da Cunha, Growth and Raman scattering characterization of Cu$_2$ZnSnS$_4$ thin films, Thin Solid Films 517 (7) (2008) 2519–2523.
[18] F. Hergert, R. Hock, Predicted formation reactions for the solid-state syntheses of the semiconductor materials Cu$_2$SnS$_3$ and Cu$_2$ZnSnX$_4$ (X= S, Se) starting from binary chalcogenides, Thin Solid Films 515 (2007) 5953–5956.
[19] H. Rodriguez-Alvarez, I.M Kotschau, H.W Schock, Pressure dependent real-time investigations on the rapid thermal sulfurization of Cu–In thin films, J. Cryst. Growth 310 (2008) 3638–3644.
[20] D.J. Chakrabarti, D.E Laughlin, The Cu-S (copper-sulfur) system, Bull. Alloy Phase Diagrams 4 (3) (1983) 254–271.
[21] S Wibmann, K.D Becker, Tracer diffusion of indium in CuInS$_2$, Solid State Ion. 101-103 (1997) 539–545.
[22] R. Scheer, I. Luck, H. Sehnert, H.J. Lewerenz, Scavenging of excess Cu atoms in CuInS$_2$ film by sulfur, Sol. Energy Mater. Sol. Cells 41–42 (1996) 261–270.
[23] C. Guillén, J. Herrero, CuInS$_2$ and CuGaS$_2$ thin films grown modulated Cu contents, Phys. Status. Solidi A 203 (10) (2006) 2438–2443.
[24] A. Catalano, Polycrystalline thin film technologies: status and prospects, Sol. Energy Mater. Sol. Cells 41–42 (1996) 205–217.
[25] R. Schurr, A. Holzing, S. Jost, R. Hock, T. Voss, J. Schulze, A. Kirbs, A. Ennaoui, M. Lux-Steiner, A Weber, I. Kotschau, H.W. Schock, The crystallization of Cu$_2$ZnSnS$_4$ thin film solar cell absorbers from co-electroplated Cu–Zn–Sn precursors, Thin Solid Films 517 (2009) 2465–2468.
[26] T. Walter, H.W. Schock, Crystal growth and diffusion in CuGaInSe$_2$ chalcopyrite thin films, Thin Solid Films 224 (1993) 74–81.
[27] O. Lundberg, J. Lu, A. Rockett, M. Edoff, L. Stolt, Diffusion of indium and gallium in Cu(In,Ga)Se2 thin film solar cells, J. Phys. Chem. Solids 64 (2003) 1499–1504.